



**HAL**  
open science

## Porcine glutathione transferase alpha 2-2 is a human GST A3-3 analogue catalyzing steroid double-bond isomerization

Natalia Fedulova, Françoise Raffalli-Mathieu, Bengt Mannervik

► **To cite this version:**

Natalia Fedulova, Françoise Raffalli-Mathieu, Bengt Mannervik. Porcine glutathione transferase alpha 2-2 is a human GST A3-3 analogue catalyzing steroid double-bond isomerization. *Biochemical Journal*, 2010, 431 (1), pp.159-167. 10.1042/BJ20100839 . hal-00517255

**HAL Id: hal-00517255**

**<https://hal.science/hal-00517255>**

Submitted on 14 Sep 2010

**HAL** is a multi-disciplinary open access archive for the deposit and dissemination of scientific research documents, whether they are published or not. The documents may come from teaching and research institutions in France or abroad, or from public or private research centers.

L'archive ouverte pluridisciplinaire **HAL**, est destinée au dépôt et à la diffusion de documents scientifiques de niveau recherche, publiés ou non, émanant des établissements d'enseignement et de recherche français ou étrangers, des laboratoires publics ou privés.

## Porcine Glutathione Transferase Alpha 2-2 is a Human GST A3-3 Analogue Catalyzing Steroid Double-Bond Isomerization

Natalia Fedulova, Françoise Raffalli-Mathieu, Bengt Mannervik\*

Department of Biochemistry and Organic Chemistry, Uppsala University, Biomedical Center, Box 576, SE-75123 Uppsala, Sweden

\*To whom correspondence should be addressed: Tel.: 46-18-471-45-39, Fax: 46-18-55-84-31, E-mail: [Bengt.Mannervik@biorg.uu.se](mailto:Bengt.Mannervik@biorg.uu.se)

Short title:

Glutathione transferase A2-2 from pig catalyzes steroid isomerisation

### SYNOPSIS

A primary role of glutathione transferases (GSTs) is detoxication of electrophilic compounds. In addition to this protective function human GST A3-3, a member of the Alpha class of soluble GSTs, has prominent steroid double-bond isomerase activity. The isomerase reaction is an obligatory step in the biosynthesis of steroid hormones, indicating a special role of human GST A3-3 in steroidogenic tissues. An analogous GST with high steroid isomerase activity has not so far been found in any other biological species. In the present investigation we characterize a *Sus scrofa* (pig) enzyme, pGSTA2-2, displaying high steroid isomerase activity. High levels of pGSTA2-2 expression were found in ovary, testis, and liver. Also in functional properties other than steroid isomerization pGSTA2-2 was similar to the human enzyme hGSTA3-3. Other human GSTs were more divergent in their functions. The properties of the novel porcine enzyme lend support to the notion that particular GSTs play an important role in steroidogenesis.

Keywords:

$\Delta^5$ -androstene-3,17-dione, androstenedione, steroidogenesis, interspecies comparison, tributyltin

Abbreviations used:

3 $\beta$ -HSD, 3 $\beta$ -hydroxysteroid dehydrogenase; 5AD,  $\Delta^5$ -androstene-3,17-dione [CAS 571-36-8]; 5PD,  $\Delta^5$ -pregnene-3,20-dione [CAS 1236-09-5];  $\beta$ ME,  $\beta$ -mercaptoethanol; Bu<sub>3</sub>SnCl, tributyltin chloride [CAS 1461-22-9]; CDNB, 1-chloro-2,4-dinitrobenzene [CAS 97-00-7]; CHP, cumene hydroperoxide [CAS 80-15-9]; DTT, dithiothreitol; EA, ethacrynic acid [CAS 58-54-8]; EtOH, ethanol; GST, glutathione transferase; Hex, trans-2-hexenal [CAS 6728-26-3]; MeCN, acetonitrile; MeOH, methanol; Non, trans-2-nonenal [CAS 30551-15-6]; PEITC, phenethyl isothiocyanate [CAS 2257-09-2].

### INTRODUCTION

Glutathione transferases (EC 2.5.1.18) of mammalia are detoxication enzymes that catalyze the conjugation of the ubiquitous tripeptide glutathione ( $\gamma$ -Glu-Cys-Gly) to exogenous and endogenous electrophiles [1-3] reacting with DNA, RNA, proteins and other essential cell components with exposed nucleophilic centers. GSTs of the Alpha, Mu and Pi classes have alternative non-enzymatic functions as ligandins [4-7] and modulators of the activity of the kinases involved in cellular signaling [8-10]. A unique feature of Alpha class GSTs is steroid isomerase activity where GSH is used as a cofactor rather than as a substrate [11] as in conjugation reactions.

Steroid hormones (mineralocorticoids, glucocorticoids, estrogens, androgens and progestagens) play crucial roles in homeostasis and development of man. Biosynthesis of steroid hormones begins with the cleavage of the cholesterol side chain and proceeds through a series of reactions dependent on pyridine nucleotides [12, 13]. Oxidation of the 3 $\beta$ -OH group in the steroid scaffold is followed by  $\Delta^5 \rightarrow \Delta^4$  double bond migration. Both these steps are indispensable steps in the production of all types of steroid hormones. Although early enzymatic studies suggested the presence of two or three pathway-specific

double-bond isomerases [mentioned in 13], it has been widely accepted that both oxidation and isomerization are catalyzed in tandem by a single enzyme 3 $\beta$ -hydroxysteroid dehydrogenase, 3 $\beta$ -HSD [14]. However, it has later been found that the most efficient *in vitro* catalyst of the double bond isomerization in  $\Delta^5$ -pregnene-3,20-dione and  $\Delta^5$ -androstene-3,17-dione is a human Alpha class GST, hGST A3-3 [15]. The corresponding mRNA has been detected in all classical steroidogenic tissues such as adrenal, mammary gland, gonads, placenta, as well as in trachea, lung, stomach, but it has not been found in thymus, liver, skeletal muscle or fetal brain [16, 15]. It has also been estimated that 74% of the steroid isomerase activity with  $\Delta^5$ -androstene-3,17-dione is GSH dependent in the human adrenocortical cell line H295R, and 10-30% of the isomerization leading progesterone in the placental choriocarcinoma cell line JEG3 is catalyzed by hGST A3-3 [17]. Hence, hGST A3-3 has been suggested to complement the activity 3 $\beta$ -HSD isomerase *in vivo*.

The aim of present study was to investigate the presence of glutathione transferases with high steroid isomerase activity in other eutherian species. The pig (*Sus scrofa*) is used as an animal model for humans in studies of, *inter alia*, the reproductive system owing to physiological similarities between the species [18]. Also, pig reproduction is being investigated because pigs remain one of the most important food sources. Many efforts have been put into breeding of sows with high reproduction efficiency and improved fertility traits [19]. Besides, steroid production is known to influence pork meat quality [20]. Thus, as complete as possible knowledge of steroidogenic pathways in pigs is desirable. On additional aspect, the presence of an analogous enzyme in another mammalian species would support the notion of a significant function of hGST A3-3 in humans. In the present study, we addressed the question whether there were GSTs in the pig that would possess significant steroid isomerase activity and act as analogues of hGST A3-3.

## EXPERIMENTAL

### *Isolation of total RNA*

Ovary and testis specimens from the domesticated Large White pig intercrossed with European Wild Boar were kindly provided by Emmanuelle Bourneuf and Leif Andersson (Department of Medical Biochemistry and Microbiology, Uppsala University, Uppsala). Total RNA was isolated from the tissues using the RNeasy Mini Kit (Qiagen), its quantity and purity were assessed spectrophotometrically and the RNA integrity was verified by denaturing electrophoresis of 4  $\mu$ g RNA according to the manufacturer's instructions.

### *cDNA synthesis*

Two  $\mu$ g total RNA was incubated with 1 U DNase I (Sigma) in a volume of 10  $\mu$ l at 22  $^{\circ}$ C for 15 min and the DNase I was inactivated by the addition of Stop Solution (Sigma) followed by heating at 70  $^{\circ}$ C for 10 min and chilling on ice. The mixture was supplemented with anchored oligo(dT)<sub>23</sub> primers (Sigma) to a final concentration of 3.5  $\mu$ M, heated at 70  $^{\circ}$ C for 10 min and chilled on ice. Then, 2  $\mu$ l 10xAMV RTase buffer (Sigma), 40 U RNase Inhibitor (Sigma), 2  $\mu$ l 10 mM dNTPs solution (Sigma) and 20 U AMV RT (Sigma) were added to the final volume of 20  $\mu$ l and incubated at 50  $^{\circ}$ C for 1 h. The reaction was stopped by heating at 85  $^{\circ}$ C for 5 min and mixtures were stored at -20  $^{\circ}$ C for subsequent pGSTA2 amplification by PCR.

### *Amplification of nucleotide sequence coding pGSTA2*

Primers for PCR amplification were 5'-TTTTTTGGATCCATATGGCGGGGAAGCCCATTCTTC and 5'-TTTTTTAAGCTTATTAACTTGAAAATCCTCC (Thermo Electron GmbH). The reaction mixture (50  $\mu$ l) included 2  $\mu$ l cDNA, 1xPhusion HF buffer (Finnzymes), 0.2 mM dNTPs (Sigma), 0.5  $\mu$ M of each primer, and 1 U Phusion DNA polymerase (Finnzymes). Three min at 98  $^{\circ}$ C were followed by 35 cycles of 98  $^{\circ}$ C for 1 min, 62  $^{\circ}$ C for 1 min, 72  $^{\circ}$ C for 1 min and, finally, by additional 10 min at 72  $^{\circ}$ C. PCR products were separated on 1.2 % agarose/TAE gel and stained with ethidium bromide. A fragment of 696 bp was isolated from the gel using QIAquick Gel Extraction kit (Qiagen), and stored at -20  $^{\circ}$ C.

#### *Construction of the cloning plasmid pGEM-3Zf(+)-pGSTA2*

The amplified pGSTA2 cDNA was digested with *Bam*HI and *Hind*III, yielding a 682 bp fragment that, after electrophoresis, was purified using QIAquick Gel Extraction kit (Qiagen). The purified DNA fragment was inserted into pGEM-3Zf(+) vector (Promega), also digested with *Bam*HI and *Hind*III, using T4 DNA ligase (Roche Applied Sciences). Electroporation-competent XL1-Blue cells (Stratagene) were transformed with the ligase mixture, and positive clones containing the pGSTA2 sequence were identified with PCR using colony lysate as a template and appropriate primers. The plasmid DNA was isolated from positive clones using Plasmid Mini kit (Qiagen), and sequenced. Sequencing was done using MegaBACE 1000 kit (GE Healthcare) at the Department of Animal Breeding and Genetics, Swedish University of Agricultural Sciences.

#### *Construction of the expression plasmid pET-21α(+)-pGSTA2*

At first, pGEM-3Zf(+)-pGSTA2 was digested with *Nde*I and a 722 bp fragment, containing the pGSTA2 sequence, was purified using QIAquick Gel Extraction kit (Qiagen). Then, this fragment was digested with *Hind*III yielding a fragment of 676 bp that was ligated into *Nde*I/*Hind*III-restricted pET-21α(+) expression vector (Novagen) using T4 DNA ligase (Roche Applied Sciences). The ligation mixture was used to transform electroporation-competent XL1-Blue cells (Stratagene), and positive clones containing pGSTA2 sequence were identified by PCR using colony lysate as a template and appropriate primers. The plasmid DNA from positive clones was isolated using Plasmid Mini kit (Qiagen), and the presence of the target pGSTA2 sequence was verified by the analysis of the size of fragments resulting from restriction of the construct with *Nde*I and *Hind*III.

#### *Expression of pGST A2-2 and hGST A3-3 in E. coli*

The pET-21α(+)-pGSTA2 plasmid was transformed into electroporation-competent Rosetta™(DE3) cells (Novagen). All cultures were grown in the presence of 100 µg/ml ampicillin and 34 µg/ml chloramphenicol at 30 °C in a shaker at 200 rpm. A starter culture of 100 ml LB medium was inoculated with single colonies of freshly transformed cells and incubated for 14 h. Three liters 2x YT medium were inoculated with starter culture as 1:50 and grown for 3 h until OD<sub>600</sub> was 0.6. Then, isopropyl-β-D-thiogalactopyranoside (Sigma) was added to a final concentration of 1 mM and incubation continued for 18 h. The cell culture was chilled on ice and then harvested at 10000 g. The cell pellets were frozen at -20 °C for subsequent protein purification. Likewise, hGST A3-3 was expressed using pET-21α(+)-hGSTA3 plasmid constructed earlier in our laboratory [21].

#### *Purification of pGST A2-2*

The cell pellet from 3 l bacterial culture was resuspended in 100 ml lysis buffer [1 mg/ml lysozyme in 0.1 M Tris-HCl pH 8.0 (0 °C), 0.1 % w/v Triton X-100, 1 mM EDTA, 14 mM βME, 0.1 % w/v polyethylene imine (Fluka), protease inhibitors (Complete EDTA-free, Roche Diagnostics GmbH)] and kept on ice for 2 h under stirring. After ultrasonication, the insoluble debris were sedimented by centrifugation. The supernatant was supplemented with (NH<sub>4</sub>)<sub>2</sub>SO<sub>4</sub> to 50 % of saturation at 0 °C, incubated for 1 h on ice, centrifuged and the pellet was discarded. The supernatant was further supplemented with (NH<sub>4</sub>)<sub>2</sub>SO<sub>4</sub> to 75 % of saturation at 0 °C, incubated for 1 h on ice and centrifuged. The supernatant was discarded and the pellet was dissolved in 8 ml starting buffer [10 mM NaCl, 20 mM Na-PO<sub>4</sub> pH 6.0 (0 °C), 13 mM βME]. The remaining (NH<sub>4</sub>)<sub>2</sub>SO<sub>4</sub> was removed by repeated gel filtration on PD-10 columns (GE Healthcare) until the conductivity was 3-4 µS/cm, similar to 3 µS/cm of the starting buffer. The solution was loaded to SP-Sepharose FF (GE Healthcare) column (3.2 cm internal diameter, bed height 13.7 cm) at 0.8 ml/min. The column was washed with 7 bed volumes of starting buffer at 0.8 ml/min. Protein was eluted from the column by gradient elution over 6 bed volumes at 0.5 ml/min; the end buffer contained 210 mM NaCl in 20 mM Na-PO<sub>4</sub> pH 6.0 (0 °C), 13 mM βME. Fractions of 6 ml were collected and the protein containing fractions were analyzed for GST activity with CDNB under standard conditions as described below. Enzymatically active fractions were pooled (250 ml) and concentrated to 9 ml by ultrafiltration on a polyethersulfone membrane with 10 kDa molecular mass cut off (Pall Life Sciences). The concentrate

was transferred to 50 ml 40 % slurry of S-hexylglutathione-Sepharose (prepared from epoxy-activated Sepharose, GE Healthcare) equilibrated with binding buffer [10 mM Tris-HCl pH 7.8 (22 °C), 5 mM  $\beta$ ME], and left on ice for 8 h. After adsorption, the gel was washed batch-wise with 4x50 ml binding buffer supplemented with 0.2 M NaCl, packed into a column (1.9 cm internal diameter), and the bound protein was eluted with 50 mM glycine-NaOH pH 10 at 1 ml/min. Fractions of 2 ml were collected into tubes already containing 0.2 ml 2 M Tris-HCl pH 7.2 (22 °C) in order to lower the pH immediately after elution. The affinity purification was repeated twice, because the gel capacity was exceeded. Protein-containing fractions were combined, dialyzed against 10 mM Tris-HCl pH 7.8 (22 °C) containing 2 mM DTT, concentrated to 39 mg/ml by ultrafiltration, aliquoted and stored at -80 °C. Enzyme purity was assessed by SDS-PAGE applying both optimal and excessive protein amounts to visualize possible impurities. For dialysis, we used regenerated cellulose tubing Spectra/Por®3 with 3.5 kDa molecular mass cut off.

#### *Purification of hGST A3-3*

Human GST A3-3 was purified with 92 mg yield from 1 l bacterial culture as follows. The cell pellet was resuspended in 50 ml lysis buffer [1 mg/ml lysozyme in 10 mM Tris-HCl pH 7.8 (22 °C), 0.1 % w/v Triton X-100, 1 mM EDTA, 14 mM  $\beta$ ME, protease inhibitors (Complete EDTA-free, Roche Diagnostics GmbH)] and kept on ice for 2 h under stirring. After ultrasonication, the cell debris were removed by centrifugation followed by filtering through 0.22  $\mu$ m Supor® membrane (Pall Life Sciences). The supernatant was added to 50 ml 20 % slurry of S-hexylglutathione-Sepharose 6B equilibrated with binding buffer [10 mM Tris-HCl pH 7.8 (22 °C), 5 mM  $\beta$ ME], and left on ice for 14 h. After adsorption, the gel was washed batch-wise with 6x50 ml binding buffer supplemented with 0.2 M NaCl, packed into a column (1 cm internal diameter) and eluted as described for pGST A2-2. The protein-containing fractions were pooled, concentrated from 50 ml to 5 ml, desalted on PD-10 columns into the 10 mM Tris-HCl pH 7.2 (22 °C) containing 5 mM  $\beta$ ME, concentrated to 47 mg/ml by ultrafiltration, aliquoted and stored at -80 °C.

#### *Determination of pI and apparent molecular mass*

Superdex 200 prep grade was packed in XK16/60 (GE Healthcare) and equilibrated with 10 mM Tris-Cl pH 7.8 containing 0.2 M NaCl at 4 °C at 0.5 ml/min. The pGST A2-2 apparent molecular mass was determined on the column using LMW Gel Filtration Calibration kit (GE Healthcare) according to the manufacturer's instructions.

The pI was determined by isoelectric focusing on precast Ampholine™ PAGplate pH 3.5-9.5 (GE Healthcare) on 2117 MULTIPHOR II Electrophoresis unit (LKB) at 10 °C using 1500 V, 50 mA, 30 W. Isoelectric Focusing Calibration Kit Broad pI (pH 3-10) (Amersham Biosciences) was used. Staining and pI calculation were performed according to the manufacturer's instructions.

#### *Kinetic characterization and inhibition studies*

The reaction rates with various substrates were followed spectrophotometrically (UV-2501PC Shimadzu, Shimadzu Inc) with an empty cell as a reference. 5AD and 5PD were purchased from Steraloids, Inc., and other substrates from Sigma-Aldrich. All substrates except GSH were dissolved in organic solvents, and, in some cases, the enzyme stock solution contained 45% glycerol (AnalaR®, BDH). The molar extinction coefficients used for calculations were  $\epsilon_{248}^{(5AD)}=16.3 \text{ mM}^{-1}\text{cm}^{-1}$ ,  $\epsilon_{248}^{(5PD)}=17.0 \text{ mM}^{-1}\text{cm}^{-1}$ ,  $\epsilon_{340}^{(CDNB)}=9.6 \text{ mM}^{-1}\text{cm}^{-1}$ ,  $\epsilon_{340}^{(CHP)}=6.2 \text{ mM}^{-1}\text{cm}^{-1}$ ,  $\epsilon_{270}^{(EA)}=5.0 \text{ mM}^{-1}\text{cm}^{-1}$ ,  $\epsilon_{224}^{(HEX)}=19.5 \text{ mM}^{-1}\text{cm}^{-1}$ ,  $\epsilon_{225}^{(NON)}=-19.22 \text{ mM}^{-1}\text{cm}^{-1}$ ,  $\epsilon_{274}^{(PEITC)}=8.89 \text{ mM}^{-1}\text{cm}^{-1}$ .

Specific activities were determined at 30 °C under the following conditions: 5AD (0.1 mM) or 5PD (0.01 mM) with 1 mM GSH, in 25 mM Na<sub>2</sub>HPO<sub>4</sub>-HCl pH 8, 5% EtOH, 0.9% glycerol; CDNB (1 mM) with 1 or 5 mM GSH, in 0.1 M KH<sub>2</sub>PO<sub>4</sub>-KOH pH 6.5, 2% EtOH; CHP (1.5 mM) with 1 or 2 mM GSH, in PBS pH 7.4, 0.3 U/ml glutathione reductase (Sigma), 0.1 mM NADPH (Sigma), 5% EtOH, 0.9% glycerol; EA (0.1 mM) with 0.25 or 2.5 mM GSH, in PBS pH 7.4, 1% MeOH; Hex (0.1 mM) with 0.5 mM GSH, in

PBS pH 7.4, 1% EtOH; Non (0.1 mM) with 0.5 mM GSH, in PBS pH 7.4, 1% EtOH, alternatively, with 1 mM GSH, in 0.1 M  $\text{KH}_2\text{PO}_4\text{-KOH}$  pH 6.5, 5% EtOH, 0.9% glycerol; PEITC (0.1 mM) with 1 mM GSH, in 0.1 M  $\text{NaH}_2\text{PO}_4\text{-NaOH}$  pH 6.5, 2% MeCN, 0.8% glycerol.

For determination of steady-state parameters, the Michaelis-Menten equation was fit to reactions rates (Simfit 6.0.28 software, W.G. Bardsley, University of Manchester) determined with fixed concentration of GSH and variable concentrations of the second substrate. Saturation curves for steady-state parameters determination were obtained at 30 °C under the following conditions (all reaction mixtures also contained 0.8-0.9% glycerol): 5AD (0.001-0.1 or 0.0005-0.1 mM) with 1 mM GSH, in 25 mM  $\text{Na}_2\text{HPO}_4\text{-HCl}$  pH 8, 1% MeOH or 5% EtOH, respectively; 5PD (0.001-0.03 mM) with 1 mM GSH, in 25 mM  $\text{Na}_2\text{HPO}_4\text{-HCl}$  pH 8, 5% EtOH; CDNB (0.002-1 mM) with 5 mM GSH or 0.001-0.2 mM Non with 1 mM GSH, in 0.1 M  $\text{KH}_2\text{PO}_4\text{-KOH}$  pH 6.5, 5% EtOH; CHP (0.025-1.5 mM) with 2 mM GSH, in PBS pH 7.4, 5% EtOH; PEITC (0.001-0.1 mM) with 1 mM GSH, in 0.1 M  $\text{NaH}_2\text{PO}_4\text{-NaOH}$  pH 6.5, 2% MeCN.

Studies of inhibition by tributyltin chloride (Aldrich) were done with 5AD and CDNB at 30 °C. For each substrate, five saturation curves were obtained in the presence of 0, 10, 20, 40, 60 nM and 120 nM inhibitor under the following conditions: 5AD (0.001-0.2 mM) with 1 mM GSH, in 25 mM  $\text{Na}_2\text{HPO}_4\text{-HCl}$  pH 8, 5% EtOH, 0.8% glycerol; CDNB (0.002-2.5 mM) with 5 mM GSH, in 0.1 M  $\text{KH}_2\text{PO}_4\text{-KOH}$  pH 6.5, 5% EtOH, 0.8% glycerol. The reaction rates obtained were processed in Prism 5.02 (GraphPad). Eadie-Hofstee plots were examined to verify that the data are described by simple hyperbolic equation. The Michaelis-Menten equation was fit to each saturation curve separately. The inhibitor concentration of 120 nM was later excluded from analysis because, due to inability to reach saturation within the solubility range of the substrate, parameters could not be determined accurately. Obtained apparent steady-state parameters were plotted versus inhibitor concentration in order to determine the inhibition type. Finally, for each substrate-enzyme combination, all reaction rates were fit simultaneously (global fit in Prism 5.02, GraphPad) to the chosen inhibition model and the parameters were determined.

#### *Expression of pGST A2-2 in various tissues*

A PCR was performed using cDNAs from ten tissues of an individual Yorkshire male pig (Zyagen) as a template. Sequence specific primers for the amplification of full-length pGSTA2 were identical to those used for cloning. For normalization of the data, a 202 bp fragment of porcine  $\beta$ -actin was amplified using primers 5'-TCCTTCCTGGGCATGGAA and 5'-GCGCGATGATCTTGATCTTCATC. The designed primers exclude amplification of non-spliced isoforms of  $\beta$ -actin as well as  $\alpha$ -actin. The mixture of 25  $\mu\text{l}$  contained 0.25  $\mu\text{l}$  template cDNA, 0.2 mM dNTPs (Sigma), 0.5  $\mu\text{M}$  of each primer, 0.01 U/ $\mu\text{l}$  Phusion DNA polymerase (Finnzymes) in 1xPhusion HF buffer. For pGSTA2 amplification, 3 min at 98 °C were followed by 34 cycles of 98 °C for 10 sec, 63 °C for 30 sec, 72 °C for 20 sec and, finally, by an additional step at 72 °C for 5 min. For  $\beta$ -actin amplification, 3 min at 98 °C were followed by 25 cycles of 98 °C for 10 sec, 60 °C for 30 sec, 72 °C for 20 sec and, finally, by additional step at 72 °C for 5 min. PCR products were separated on 2 % agarose/TBE gel, stained with ethidium bromide and a photo was taken. Primer specificity was confirmed by sequencing of PCR fragments from liver and testis. For quantification, the intensity of PCR fragments was evaluated using Image J 1.33u software (NIH). Intensities of pGSTA2 PCR fragments were normalized to the intensities of  $\beta$ -actin bands from the corresponding tissues and to the intensity of the pGSTA2 band from liver. The resulting normalized intensity values were assigned to an ordinal scale as follows: (0; 0.1) = +, [0.1; 0.5) = ++, [0.5; 1) = +++.

## RESULTS

### *Choice of porcine glutathione transferase potentially active as a steroid isomerase*

A BLASTP [SIB BLAST Network service] search restricted to mammalia was performed against the UniProtKB using the amino acid sequence of hGST A3-3 (Swiss-Prot: Q16772) as a query. Five porcine amino acid sequences were retrieved, Swiss-Prot: P51781, P80031 and TrEMBL: Q29057, Q29581, Q29188 (**Supplemental Figure 1**). In the present study, we chose a putative glutathione transferase, entry

Q29057, for which an mRNA transcript has been identified as involved in pig ovarian follicular differentiation [22]. The sequence was assigned to the Alpha class due to 84 % amino acid identity to hGST A3-3 (**Figure 1**). In accordance with the latest convention on glutathione transferases nomenclature [23, 24], we refer to this enzyme as porcine glutathione transferase Alpha 2-2, pGST A2-2. When many organisms are considered, this enzyme should be referred to as *Ssc*GST A2-2 where *Ssc* represents the *Sus scrofa* species.

#### *Molecular cloning of pGSTA2 cDNA*

Porcine GSTA2 cDNA was cloned from ovary as well as from testis. Total RNA was isolated from the tissues and cDNA was synthesized using anchored oligo(dT)<sub>23</sub>. PCR fragments were amplified using pGSTA2 specific primers and inserted into the pGEM-3Zf(+) cloning vector. Porcine GSTA2 cDNAs cloned from both ovary and testis were sequenced and showed identity with the pGSTA2 sequence published in the data base. The pGSTA2 cDNA was successfully subcloned into the pET-21α(+) vector for overexpression in *E. coli*.

#### *Heterologous expression and purification of pGST A2-2*

Porcine GST A2-2 was expressed in the *E. coli* Rosetta™(DE3) strain and purified to homogeneity. A purification method involving fractional ammonium sulfate precipitation, SP-Sepharose cation-exchange and S-hexylglutathione affinity chromatographies was developed in order to obtain pGST A2-2 of the purity and quantity necessary for crystallization trials. This three-step purification procedure yielded 150 mg of high purity pGST A2-2 from 3 l culture. Other purification approaches were not as efficient. The widely used glutathione affinity chromatography yielded only 11.2 mg protein from 3 l bacterial culture, because the bulk of the overexpressed enzyme did not bind to the chromatography medium, but appeared in the flow through. Alternatively, up to 32 mg enzyme were obtained from 1 l culture using CM-Sepharose. It should also be mentioned that pH 6 as well as very low ionic strength were necessary for complete adsorption of pGST A2-2 to a cation-exchanger (**Supplemental Figure 2**).

#### *Characterization of basic physical properties and catalytic activities of pGST A2-2*

Porcine GST A2-2 contains 223 amino acid residues including the initial Met. The molecular mass of the pGST A2 subunit is 25.4 kDa, but the protein is a dimer with an apparent molecular mass of 40 kDa as determined by gel filtration. The molar extinction coefficient of 18.91 mM<sup>-1</sup>cm<sup>-1</sup> and Abs<sup>0.1%</sup> of 0.745 at 280 nm, assuming both cysteines (Cys18 and Cys112) are reduced, were calculated by ProtParam tool and used to determine the enzyme concentration. The isoelectric point at pH 9.15 (10 °C) was determined experimentally by isoelectric focusing. The specific activities of pGST A2-2 with several substrates were measured under standard conditions (**Table 1**). The enzyme demonstrated the highest specific activity of 53 μmol/min per mg with 5AD, moderate activity with CDNB and PEITC (14 and 13 μmol/min per mg, respectively), while activities with CHP, 5PD, Non, Hex and EA did not exceed 4.2 μmol/min per mg. Normalizing all values obtained in the presence of 1 mM GSH (or approximated to the presence of 1 mM GSH) to the specific activity with 5AD (100%), it appears that pGST A2-2 shows 25% activity with CDNB and PEITC, and less than 4% activity with CHP, 5PD, Non, Hex and EA.

#### *Steady-state kinetic parameters of pGST A2-2*

Steady-state parameters were determined with various substances (**Table 2**) characterized as substrates for pGST A2-2: 5AD, 5PD, CDNB, CHP, Non and PEITC (**Figure 2**). All parameters were measured at the saturating concentration of glutathione of 1-5 mM and no more than 1.5 mM concentration of the variable substrate. The concentration used was limited either by the solubility of the electrophile or the high rate of the non-enzymatic reaction. Porcine GST A2-2 obeyed Michaelis-Menten kinetics under the conditions used. The specificity constant  $k_{\text{cat}}/K_M$  and the Michaelis constant obtained with 5AD, the most active substrate, were about 1600 mM<sup>-1</sup>s<sup>-1</sup> and 25 μM, respectively. 5PD has a lower  $K_M$  of 9 μM, which points to it as another preferable substrate even though its catalytic constant is only 1.5 s<sup>-1</sup> ( $k_{\text{cat}}/K_M$  is 170 mM<sup>-1</sup>s<sup>-1</sup>). PEITC has  $k_{\text{cat}}/K_M$  value of 150 mM<sup>-1</sup>s<sup>-1</sup> similar to that of 5PD. The Michaelis constants for the

naturally occurring PEITC, Non and both steroids are below 60  $\mu\text{M}$ , while the  $K_M$  values for the artificial substrates CDNB and CHP exceed 300  $\mu\text{M}$ . CHP also has a low  $k_{\text{cat}}$  of 2.5  $\text{s}^{-1}$ , which in combination with the  $K_M$  value makes it a poor substrate.

#### *Inhibition characteristics of pGST A2-2 and hGST A3-3*

Inhibition studies were performed on pGST A2-2 and hGST A3-3 using tributyltin chloride – an inhibitor of steroidogenesis [25-28]. Both pGST A2-2 and hGST A3-3 were found to be competitively inhibited by  $\text{Bu}_3\text{SnCl}$  in reaction with 5AD, since  $V_{\text{max}}^{\text{app}}$  was independent on the inhibitor concentration (**Supplemental Figure 3**). The inhibition constants obtained with 5AD are 30 nM for pGST A2-2 and 78 nM for hGST A3-3 (**Table 3**). Using CDNB as substrate,  $\text{Bu}_3\text{SnCl}$  gave rise to increasing  $K_M^{\text{app}}$  and decreasing  $V_{\text{max}}^{\text{app}}$ . The data were best described by the mixed inhibition rather than the noncompetitive model since the  $\alpha$  coefficients were not equal to 1 for any of the enzymes. For pGST A2-2 and hGST A3-3,  $K_i^{\text{CDNB}}$  were determined as 22 nM and 25 nM, respectively (**Table 3**).

#### *Tissue expression of pGST A2-2*

During the molecular cloning experiment, expression of pGSTA2 mRNA in ovary appeared to be at a level similar to that in testis. The molecular cloning from both ovary and testis was performed in parallel using the same amount of mRNA/cDNA template for final PCR intended for full-length pGSTA2 cDNA amplification. PCR products from the two tissues appeared on agarose gel as bands with high intensities (**Figure 3A**). To investigate further whether pGST A2-2 is expressed in tissues of major steroid hormones synthesis, the presence of pGSTA2 mRNA was tested in ten porcine tissues (**Figure 3B**) using sequence specific primers. We verified that primers did not crossamplify any similar GST by sequencing of the obtained PCR fragments. We also verified that the primers did not amplify another GST by using the very similar pGST A1-1 sequence as a template. The most intensive signals were detected in liver and testis. Pituitary, skin and kidney displayed weak signals. No pGSTA2 mRNA was observed in adipose tissue, adrenal, brain, lung and prostate. Neither in molecular cloning experiments nor in studying the expression profile were tissue or gender polymorphisms detected by sequencing.

## DISCUSSION

#### *Significant steroid isomerase activity positions pGST A2-2 between hGST A3-3 and A1-1*

Androstenedione (5AD) is a precursor of sex steroid hormones in males and females. Its synthesis from pregnenolone requires double-bond steroid isomerization activity that is catalyzed by  $3\beta$ -HSD complemented by hGST A3-3 in humans [17]. Among eutheria, hGST A3-3 has the highest isomerase activity so far discovered. The  $k_{\text{cat}}/K_M$  value with 5AD has been reported as 3600-5000  $\text{mM}^{-1}\text{s}^{-1}$  [15, 21, 29]. The  $k_{\text{cat}}/K_M$  value for hGST A1-1, the second highest isomerase activity in humans, is significantly lower at 180-980  $\text{mM}^{-1}\text{s}^{-1}$  [11, 29, 30]. The isomerase activity of the porcine enzyme pGST A2-2, cloned and characterized in this study, is intermediate between these values,  $k_{\text{cat}}/K_M$  is 960-2300  $\text{mM}^{-1}\text{s}^{-1}$ . The major contribution to the differences in activity of hGST A1-1, A3-3, pGST A2-2 as well as bGST A1-1 [31] is found in  $k_{\text{cat}}$  varying > 100 fold, whereas  $K_M$  differs < 10 fold. The catalytic activities with 5PD for these enzymes are lower, but the ranking of the relative activities is the same as with 5AD (**Figure 2**).

Human  $3\beta$ -HSDs are less catalytically efficient. With 5AD,  $k_{\text{cat}}/K_M$  of human  $3\beta$ -HSD type 2 and type 1 is 0.6 % and 0.3 % of hGST A3-3, respectively [32, 33]. With 5PD,  $k_{\text{cat}}/K_M$  of human  $3\beta$ -HSD type 1 is 4 % of hGST A3-3 [33]. Porcine  $3\beta$ -HSD isomerase activity has not been measured yet. For comparison,  $(k_{\text{cat}}/K_M)^{5\text{AD}}$  of human  $3\beta$ -HSD2 does not exceed 2 % of that for pGST A2-2 [32]. *In vivo* though,  $3\beta$ -HSDs have been shown to be the major steroid isomerases presumably due to membrane localization [14] and the contribution of pGST A2-2 to steroidogenesis *in vivo* is yet to be studied.

#### *Catalytic efficiency profiles reveal pGST A2-2 similarity to hGST A3-3*

In order to assess whether pGST A2-2 is a functional analogue of a human Alpha GST, we compared its steady-state parameters for six substrates representing different types of chemistry (**Figure 2**). Although catalytic properties of human Alpha class GSTs have not been systematically compared, many reported

kinetic measurements provide insight into the catalytic activity of the enzymes. Due to low activity with 5AD relative to other substrates, neither hGST A2-2 [11, 34, 35] nor hGST A4-4 [30, 34, 36, 37] can be considered as analogues of pGST A2-2. Human GST A5-5 has been poorly characterized so far and it is not yet clear whether it is expressed *in vivo* at all [38]. Prominent catalytic efficiencies with 5AD and 5PD position pGST A2-2 substrate preference between those of hGST A1-1 and A3-3 (**Figure 2**). However, the higher  $k_{cat}/K_M$  for PEITC over CDNB as well as CHP indicates that pGST A2-2 follows the catalytic efficiency profile of hGST A3-3 rather than hGST A1-1.

#### *Inhibition studies point to resemblance of pGST A2-2 and hGST A3-3*

Tributyltin chloride ( $Bu_3SnCl$ ) is a ubiquitous contaminant whose detrimental effects on growth and steroid hormone production have been shown in mice [25], rats [26], cattle [27], and pigs [28]. Human GST A3-3 and pGST A2-2 showed decreased activity in the presence of  $Bu_3SnCl$ . Besides, the type of inhibition was shown to be similar between these enzymes (**Table 3**). The inhibition of 5AD isomerisation was competitive, while the inhibition of CDNB conjugation was of mixed type. Knowing that both 5AD and CDNB bind in the H-site and that CDNB is less bulky than 5AD, it can be assumed that the uncompetitive component appears when the inhibitor binds to the H-site together with CDNB forming a dead-end complex. The larger 5AD molecule may prevent simultaneous binding of the inhibitor. The  $\alpha^{CDNB}$  coefficient for pGST A2-2 is half of  $\alpha^{CDNB}$  for hGST A3-3 (5 respective 10), implying that pGST A2-2 H-site accommodates the inhibitor into GST/GSH/CDNB complex more readily and might be more spacious than that of hGST A3-3. The strength of inhibition was found to be similar for both enzymes although, in the case of 5AD,  $K_i$  of pGST A2-2 is half of that for hGST A3-3, implying that pGST A2-2 is more susceptible than hGST A3-3 to inhibition of the isomerisation reaction by  $Bu_3SnCl$ .

#### *Tissue expression of pGST A2-2 coincides with steroid biosynthesis profile*

Porcine GST A2-2 expression was detected in gonads. In combination with high steroid isomerase activity of the enzyme, it strengthens the notion that pGST A2-2 contributes to sex steroid production *in vivo*. Porcine GST A2-2 expression pattern apparently shares features of both hGST A1-1 and hGST A3-3. Porcine GST A2-2 mRNA biosynthesis is rather tissue selective like that of hGST A3-3 or hGST A1-1/A2-2 whereas hGST A4-4 biosynthesis is ubiquitous [16]. On the other hand, the hGSTA3-3 transcript is a subject to alternative splicing [15, 16], which we did not observe for pGST A2-2. Human GST A2-2 expression appears to be less related to steroidogenic tissues than hGST A1-1, being absent in placenta and mammary gland. Otherwise the hGST A2-2 mRNA profile is very similar to hGST A1-1 with expression occurring selectively [16]. In contrast to hGST A3-3, pGST A2-2 was found to be expressed in liver. However,  $3\beta$ -HSD has also been detected in porcine liver on the mRNA [39] and the protein [40] levels suggesting that its activity may be complemented by pGST A2-2 in this tissue. Low expression of pGST A2-2 in kidney, skin and pituitary is consonant with low steroid production outside the steroidogenic centers. For example in humans,  $3\beta$ -HSD type 1 is expressed in skin, liver and other peripheral tissues [12-14]. Porcine GST A2-2 expression in liver and kidney may also be interesting due to its considerable PEITC conjugation activity. PEITC has been shown to inhibit the growth of breast [41] and ovarian [42] cancer cells in humans at the nutritionally relevant concentrations. The growth inhibition functions via downregulation of estrogen receptor  $\alpha$  expression, which abrogates mitogenic estrogen signaling [43]. Therefore, contribution to sex steroid production as well as neutralization of PEITC by pGST A2-2 and hGST A3-3 might be important for the development of steroid-dependent cancer cells.

#### *Amino acid sequence comparison reveals clusters of variable residues*

Porcine GST A2-2 shares 84 % identical amino acid residues with hGST A3-3 (**Figure 1**). Amino acid residues differing pGST A2-2 from hGST A3-3 are nonuniformly distributed and rather clustered at three regions (**Dashed boxes on Figure 1**): 7 of 10 differences in the N-terminal thioredoxin domain are located within the Glu36-Leu51 region, 9 of 15 substitutions in the C-terminal domain range from Pro113 to Lys141, and the terminal 17 residues include 8 substitutions. As shown in **Figure 1**, those regions of

residue variability involve H-site and, to a less extent, G-site. The first cluster of variable residues spans the  $\alpha 2$  helix situated between the  $\beta$ -sheet and the end of the helix  $\alpha 9$  on the surface. In human Alpha class GSTs, its residue Arg45 forms a salt-bridge with the carboxy-terminus of GSH. In pGST A2-2, Thr45 could form the H-bond to Gln53 but is out of reach for GSH, which might affect GSH binding. The second cluster of variable residues (including Arg131 conserved for GSH binding) is located in the helix  $\alpha 5$  situated on the edge of the second monomer on the other side of the active site at the  $90^\circ$  angle to  $\alpha 9$  helix. All variable residues are either on the surface or conservative and do not seem to disturb  $\alpha 4$  and  $\alpha 5$  helices arrangement. The third cluster of variable residues includes the terminal helix  $\alpha 9$  confining the H-site and contains the only two residues discriminating the H-site of pGST A2-2 from that of hGST A3-3.

#### *Structure-function relationships for isomerase activity*

Porcine GST A2-2 shares 84 % sequence identity with hGST A3-3 (**Figure 1**). However, absolute isomerase activity value or its ratio to other substrates cannot be predicted based on overall identity. For example,  $(k_{cat}/K_M)^{5AD}$  of hGST A1-1 and hGST A2-2/Penta mutant [34] are half respective two-folds that of pGST A2-2 (**Figure 2**) [11, 29, 30], while both share 91 % identity with hGST A3-3.

Steroid bound in the H-site of hGST A3-3 may interact with 17 amino acid residues as deduced from the crystal structures (**Figure 1**) [29, 44]. For all characterized Alpha GSTs including its mutants (with only exception for hGST A3-3/Triple mutant [21]), increasing the number of differences from the H-site of hGST A3-3 lowers the catalytic efficiency of the GSTs. All H-site residues of pGST A2-2 except for Thr208 and Ser212 are identical with those of hGST A3-3. The residues, that are both Ala in hGST A3-3, surround 17-carbonyl of 5AD and seem to account for 2/3 loss in  $(k_{cat}/K_M)^{5AD}$  of pGST A2-2. Bulkier polar side chains directed towards the center of the steroid binding cavity could affect both  $K_M$ , by decreasing the hydrophobicity of the H-site, and  $k_{cat}$ , by changing the the 5AD positioning relative to GSH and Tyr9 involved in catalysis [21]. It is interesting though, that in bGST A1-1, where residue 212 is long and basic Lys,  $K_M^{5AD}$  is lowest of all steroids and all Alpha GSTs [31]. Also in hGST A4-4 containing Tyr212,  $K_M^{5AD}$  is no more than that of hGST A1-1 with Ser212. The fact that neither Lys nor Tyr in position 212 abolish 5AD binding may be explained by the hGST A1-1 structure: Ser212 in hGST A1-1 points outwards the active site and is exposed to solvent (PDB ID: 1GSF and 1PKW). Ala in position 208 has been identified as preferential over Met for isomerase activity of hGST A2-2 [34]. As can be concluded from the crystal structures available for hGST A1-1 and A3-3 (PDB ID: 2VCV and 1TDI),  $\beta$ -branched Thr208 of pGST A2-2 could be even less tolerated than Met208 due to its limited rotational freedom around  $C\alpha$ - $C\beta$  bond. Isomerase activity of pGST A2-2 is nevertheless higher than that of hGST A1-1.

The polypeptide chain portions in close proximity to bound GSH are highly conserved in Alpha class GSTs. But, G-site residues themselves may vary (Leu41 and Val66 on **Figure 1**) indicating that juxtaposition of activated GSH and a steroid substrate in the active site may be disturbed by the overall GST molecule distortion. Conformational plasticity, reported to correlate with high promiscuity of Alpha class GSTs [45], makes prediction of high isomerase activity in GSTs challenging.

#### *In conclusion*

Our study provides evidence that porcine GST A2-2 is an analogue of human GST A3-3. These enzymes are similar in several aspects: high steroid isomerase activity and selective expression pattern, susceptibility to inhibition by the endocrine disruptor tributyltin, as well as similarity of kinetic parameters with representative substrates. At the same time, the existence of steroidogenic GSTs both in pig and in human provides further evidence in favor of the physiological significance of steroid isomerase activity of GSTs in eutheria.

Acknowledgements:

We thank Emmanuelle Bourneuf and Leif Andersson for tissue specimens of pig ovary and testis. Mikael Widersten is acknowledged for valuable comments on the manuscript.

#### Funding:

This work was supported by the Herbert and Karin Jacobssons foundation and the Swedish Cancer Society.

#### REFERENCES

- 1 Eaton, D.L., Bammler, T.K. (1999) Concise review of the glutathione S-transferases and their significance to toxicology. *Toxicol. Sci.* **49**, 156-164
- 2 Frova, C. (2006) Glutathione transferases in the genomic era: new insights and perspectives. *Biomol. Eng.* **23**, 149-169
- 3 Josephy, P.D., Mannervik, B. (2006) *Molecular toxicology (Second edition)*, pp. 303-401, Oxford University Press, Inc., New York
- 4 Habig, W.H., Pabst, M.J., Fleischner, G., Gatmaitan, Z., Arias, I.M., Jakoby, W.B. (1974) The identity of glutathione S-transferase B with ligandin, a major binding protein of liver. *Proc. Natl. Acad. Sci. USA* **71**, 3879-3882
- 5 Litwack, G., Ketterer, B., Arias, I.M. (1971) Ligandin: a hepatic protein which binds steroids, bilirubin, carcinogens and a number of exogenous organic anions. *Nature*. **234**, 466-467
- 6 Arias, I.M., Ohmi, N., Bhargava, M., Listowsky, I. (1980) Ligandin: an adventure in liverland. *Mol. Cell. Biochem.* **29**, 71-80
- 7 Caccuri, A.M., Aceto, A., Piemonte, F., Di Ilio, C., Rosato, N., Federici, G. (1990) Interaction of hemin with placental glutathione transferase. *Eur. J. Biochem.* **189**, 493-507
- 8 Romero, L., Andrews, K., Ng, L., O'Rourke, K., Maslen, A., Kirby, G. (2006) Human GSTA1-1 reduces c-Jun N-terminal kinase signalling and apoptosis in Caco-2 cells. *Biochem. J.* **400**, 135-141
- 9 Cho, S.G., Lee, Y.H., Park, H.S., Ryoo, K., Kang, K.W., Park, J., Eom, S.J., Kim, M.J., Chang, T.Sh., Choi, S.Y., Shim, J., Kim, Y., Dong, M.S., Lee, M.J., Kim, S.G., Ichijo, H., Choi, E.J. (2001) Glutathione S-transferase Mu modulates the stress-activated signals by suppressing apoptosis signal-regulating kinase 1. *J. Biol. Chem.* **276**, 12749-12755
- 10 Adler, V., Yin, Zh., Fuchs, S.Y., Benezra, M., Rosario, L., Tew, K.D., Pincus, M.R., Sardana, M., Henderson, C.J., Wolf, C.R., Davis, R.J., Ronai, Z. (1999) Regulation of JNK signaling by GSTp. *EMBO J.* **18**, 1321-1334
- 11 Pettersson, P.L., Mannervik, B. (2001) The role of glutathione in the isomerization of  $\Delta^5$ -androstene-3,17-dione catalyzed by human glutathione transferase A1-1. *J. Biol. Chem.* **276**, 11698-11704
- 12 Payne, A.H., Hales, D.B. (2004) Overview of steroidogenic enzymes in the pathway from cholesterol to active steroid hormones. *Endocr. Rev.* **25**, 947-970
- 13 Miller, W.L. (1988) Molecular biology of steroid hormone synthesis. *Endocr. Rev.* **9**, 295-318
- 14 Simard, J., Ricketts, M.-L., Gingras, S., Soucy, P., Feltus, A., Melner, M.H. (2005) Molecular biology of the  $3\beta$ -hydroxysteroid dehydrogenase/ $\Delta^5$ - $\Delta^4$  isomerase gene family, *Endocr. Rev.* **26**, 525-582
- 15 Johansson, A.-S., and Mannervik, B. (2001) Human glutathione transferase A3-3, a highly efficient catalyst of double-bond isomerization in the biosynthetic pathway of steroid hormones. *J. Biol. Chem.* **276**, 33061-33065
- 16 Morel, F., Rauch, C., Coles, B., Le Ferrec, E., Guillouzo, A. (2002) The human glutathione transferase alpha locus: genomic organization of the gene cluster and functional characterization of the genetic polymorphism in the hGSTA1 promoter. *Pharmacogenetics* **12**, 277-286
- 17 Raffalli-Mathieu, F., Orre, C., Stridsberg, M., Hansson Edalat, M., and Mannervik, B. (2008) Targeting human glutathione transferase A3-3 attenuates progesterone production in human steroidogenic cells. *Biochem. J.* **414**, 103-109

- 18 Lunney, J.K. (2007) Advances in swine biomedical model genomics. *Int. J. Biol. Sci.* **3**, 179-184
- 19 Spötter, A., Distl, O. (2006) Genetic approaches to the improvement of fertility traits in the pig. *Vet. J.* **172**, 234-247
- 20 Robic, A., Larzul, C., Bonneau, M. (2008) Genetic and metabolic aspects of androstenone and skatole deposition in pig adipose tissue: a review. *Genet. Sel. Evol.* **40**, 129-143
- 21 Johansson, A.S., Mannervik, B. (2002) Active-site residues governing high steroid isomerase activity in human glutathione transferase A3-3. *J. Biol. Chem.* **277**, 16648-16654
- 22 Tosser-Klopp, G., Benne, F., Bonnet, A., Mulsant, P., Gasser, F., Hatey, F. (1997) A first catalog of genes involved in pig ovarian follicular differentiation. *Mamm. Genome* **8**, 250-254
- 23 Mannervik, B., Board, P.G., Hayes, J.D., Listowsky, I., Pearson, W.R. (2005) Nomenclature for mammalian soluble glutathione transferases. *Methods Enzymol.* **401**, 1-8
- 24 Mannervik, B., Awasthi, Y.C., Board, P.G., Hayes, J.D., Di Ilio, C., Ketterer, B., Listowsky, I., Morgenstern, R., Muramatsu, M., Pearson, W.R., Pickett, C.B., Sato, K., Widersten, M., Wolf, C.R. (1992) Nomenclature for human glutathione transferases. *Biochem. J.* **282**, 305-306
- 25 Kim, S.-K., Kim, J.-H., Han, J.H., Yoon, Y.-D. (2008) Inhibitory effect of tributyltin on expression of steroidogenic enzymes in mouse testis. *Int. J. Toxicol.* **27**, 175-182
- 26 McVey, M.J., Cooke, G.M. (2003) Inhibition of rat testis microsomal  $3\beta$ -hydroxysteroid dehydrogenase activity by tributyltin. *J. Steroid Biochem. Mol. Biol.* **86**, 99-105
- 27 Yamazaki, T., Shimodaira, M., Kuwahara, H., Wakatsuki, H., Horiuchi, H., Matsuda, H., Kominami, S. (2005) Tributyltin disturbs bovine adrenal steroidogenesis by two modes of action. *Steroids* **70**, 913-921
- 28 Ohno, S., Nakajima, Y., Nakajin, S. (2005) Triphenyltin and tributyltin inhibit pig testicular  $17\beta$ -hydroxysteroid dehydrogenase activity and suppress testicular testosterone biosynthesis. *Steroids* **70**, 645-651
- 29 Gu, Y., Guo, J., Pal, A., Pan, S.S., Zimniak, P., Singh, S.V., Ji, X. (2004) Crystal structure of human glutathione S-transferase A3-3 and mechanistic implications for its high steroid isomerase activity. *Biochemistry* **43**, 15673-15679
- 30 Gustafsson, A., Nilsson, L.O., Mannervik, B. (2002) Hybridization of alpha class subunits generating a functional glutathione transferase A1-4 heterodimer. *J. Mol. Biol.* **316**, 395-406
- 31 Raffalli-Mathieu, F., Persson, D., Mannervik, B. (2007) Differences between bovine and human steroid double-bond isomerase activities of Alpha-class glutathione transferases selectively expressed in steroidogenic tissues. *Biochim. Biophys. Acta* **1770**, 130-136
- 32 Thomas, J.L., Mack, V.L., Glow, J.A., Moshkelani, D., Terrell, J.R., Bucholtz, K.M. (2008) Structure/function of the inhibition of human  $3\beta$ -hydroxysteroid dehydrogenase type 1 and type 2 by trilostane. *J. Steroid Biochem. Mol. Biol.* **111**, 66-73
- 33 Thomas, J.L., Myers, R.P., Strickler, R.C. (1989) Human placental  $3\beta$ -hydroxy-5-ene-steroid dehydrogenase and steroid  $5\rightarrow 4$ -ene-isomerase: purification from mitochondria and kinetic profiles, biophysical characterization of the purified mitochondrial and microsomal enzymes. *J. Steroid Biochem.* **33**, 209-217
- 34 Pettersson, P.L., Johansson, A.S., Mannervik, B. (2002) Transmutation of human glutathione transferase A2-2 with peroxidase activity into an efficient steroid isomerase. *J. Biol. Chem.* **277**, 30019-30022
- 35 Tetlow, N., Board, P.G. (2004) Functional polymorphism of human glutathione transferase A2. *Pharmacogenetics* **14**, 111-116
- 36 Board, P.G. (1998) Identification of cDNAs encoding two human Alpha class glutathione transferases (GSTA3 and GSTA4) and the heterologous expression of GSTA4-4. *Biochem. J.* **330**, 827-831
- 37 Hubatsch, J., Ridderström, M., Mannervik, B. (1998) Human glutathione transferase A4-4: an Alpha class enzyme with high catalytic efficiency in the conjugation of 4-hydroxynonenal and other genotoxic products of lipid peroxidation. *Biochem. J.* **330**, 175-179

- 38 Singh, Sh.P., Zimniak, L., Zimniak, P. (2010) The human hGSTA5 gene encodes an enzymatically active protein. *Biochim. Biophys. Acta* **1800**, 16-22
- 39 Chen, G., Bourneuf, E., Marklund, S., Zamaratskaia, G., Madej, A., Lundström, K. (2007) Gene expression of 3 $\beta$ -hydroxysteroid dehydrogenase and 17 $\beta$ -hydroxysteroid dehydrogenase in relation to androstenedione, testosterone, and estrone sulphate in gonadally intact male and castrated pigs. *J. Anim. Sci.* **85**, 2457-2463
- 40 Furster, C. (1999) Hepatic and extrahepatic dehydrogenation/isomerization of 5-cholestene-3 $\beta$ ,7 $\alpha$ -diol: localization of 3 $\beta$ -hydroxy- $\Delta^5$ -C<sub>27</sub>-steroid dehydrogenase in pig tissues and subcellular fractions. *Biochim. Biophys. Acta* **1436**, 343-353
- 41 Tseng, E., Scott-Ramsay, E.A., Morris, M.E. (2004) Dietary organic isothiocyanates are cytotoxic in human breast cancer MCF-7 and mammary epithelial MCF-12A cell lines. *Exp. Biol. Med. (Maywood)* **229**, 835-842
- 42 Satyan, K.S., Swamy, N., Dizon, D.S., Singh, R., Granai, C.O., Brard, L. (2006) Phenethyl isothiocyanate (PEITC) inhibits growth of ovarian cancer cells by inducing apoptosis: Role of caspase and MAPK activation. *Gynecol. Oncol.* **103**, 261-270
- 43 Kang, L., Wang, Z.Y. (2009) Breast cancer cell growth inhibition by phenethyl isothiocyanate is associated with downregulation of estrogen receptor- $\alpha$ 36. *J. Cell Mol. Med.* doi:10.1111/j.1582-4934.2009.00877.x
- 44 Tars, K., Olin, B., Mannervik, B. (2010) Structural basis for featuring of steroid isomerase activity in alpha class glutathione transferases. *J. Mol. Biol.* **397**, 332-340
- 45 Hou, L., Honaker, M.T., Shireman, L.M., Balogh, L.M., Roberts, A.G., Ng, K.C., Nath, A., Atkins, W.M. (2007) Functional promiscuity correlates with conformational heterogeneity in A-class glutathione S-transferases. *J Biol. Chem.* **282**, 23264-23274
- 46 Porollo, A., Adamczak, R., Meller, J. (2004) POLYVIEW: A flexible visualization tool for structural and functional annotations of proteins. *Bioinformatics* **20**, 2460-2462
- 47 Lien, S., Gustafsson, A., Andersson, A.K., Mannervik B. (2001) Human glutathione transferase A1-1 demonstrates both half-of-the-sites and all-of-the-sites reactivity. *J. Biol. Chem.* **276**, 35599-35605
- 48 Kolm, R.H., Danielson, U.H., Zhang, Y., Talalay, P., Mannervik, B. (1995) Isothiocyanates as substrates for human glutathione transferases: structure-activity studies. *Biochem. J.* **311**, 453-459
- 49 Stenberg, G., Board, P.G., Carlberg, I., Mannervik, B. (1991) Effects of directed mutagenesis on conserved arginine residues in a human class Alpha glutathione transferase. *Biochem. J.* **274**, 549-555
- 50 Tetlow, N., Coggan, M., Casarotto, M.G., Board, P.G. (2004) Functional polymorphism of human glutathione transferase A3: effects on xenobiotic metabolism and steroid biosynthesis. *Pharmacogenetics* **14**, 657-663

## TABLES:

**Table 1.** Specific activities of pGST A2-2 with various substrates.

Substrate	$\mu\text{mol}/\text{min}$ per mg	[S] mM	[GSH] mM	pH	[pGSTA2] nM
5AD	53±2	0.1	1	8	3
CDNB	29±3	1	5	6.5	63
	14±1				
PEITC	13±1	0.1	1	6.5	54
CHP	4.2±0.1	1.5	2	7.4	319
	2.2±0.2				
5PD	1.9±0.1	0.01	1	8	20
Non	1.6±0.2	0.1	1	6.5	136
	1.2±0.2				
Hex	0.90±0.05	0.1	0.5	7.4	97
	0.11±0.02				
EA	0.056±0.009	0.1	2.5	7.4	969

**Table 2.** Steady-state parameters of pGST A2-2 with various substrates.

Substrate	$k_{\text{cat}}/K_M$ $\text{mM}^{-1}\text{s}^{-1}$	$k_{\text{cat}}$ $\text{s}^{-1}$	$K_M$ $\mu\text{M}$	[pGSTA2] nM
5AD	1600*	40*	25*	
	$\begin{pmatrix} 2300 \pm 200 \\ 960 \pm 50 \end{pmatrix}$	$\begin{pmatrix} 43 \pm 2 \\ 29 \pm 1 \end{pmatrix}$	$\begin{pmatrix} 19 \pm 2 \\ 31 \pm 2 \end{pmatrix}$	$\begin{pmatrix} 2 \\ 3 \end{pmatrix}$
5PD	170±20	1.5±0.1	9±1	20
PEITC	150±15	7.8±0.4	53±5	54
CDNB	46±2	17±1	375±14	65
Non	36±3	0.91±0.04	35±4	136
CHP	4.7±0.3	2.5±0.1	532±29	319

\* mean of two values in parenthesis. The values were determined in different experiments.

**Table 3.** Inhibition of pGST A2-2 and hGST A3-3 with  $\text{Bu}_3\text{SnCl}$  in reaction with 5AD or CDNB.

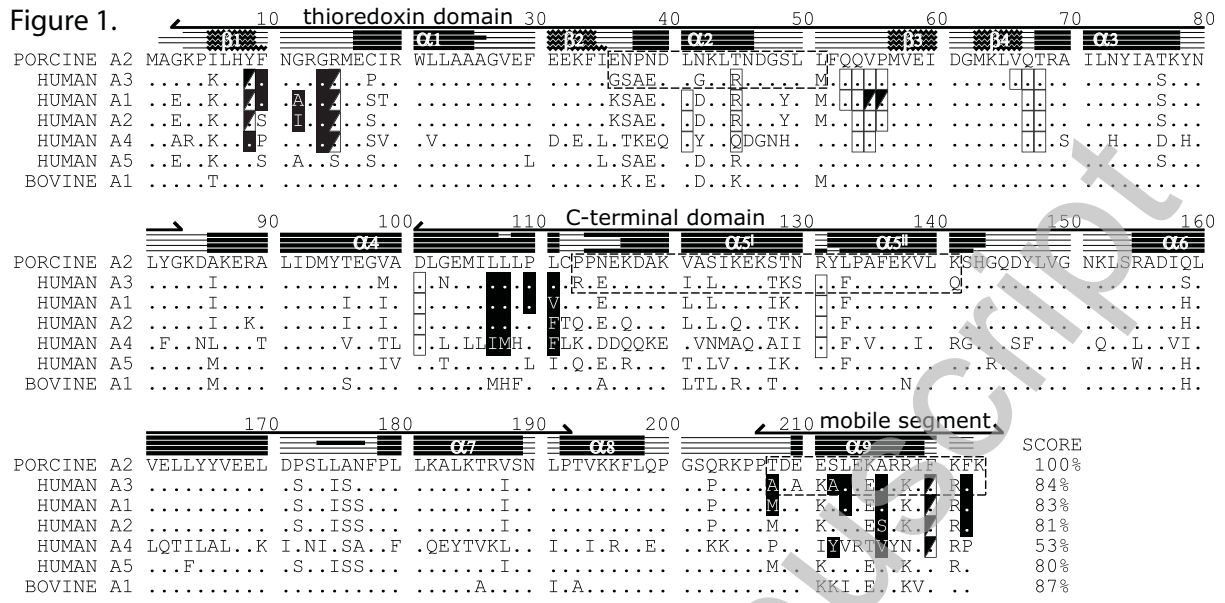
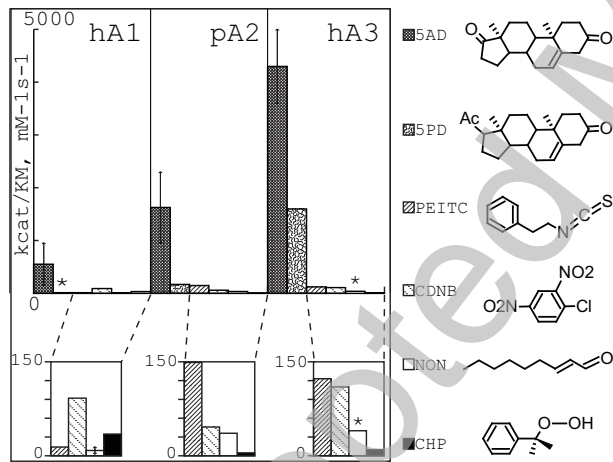
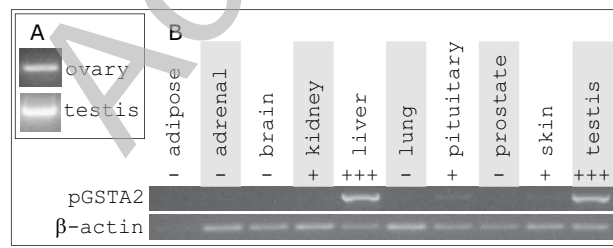
Enzyme	pGST A2-2	hGST A3-3	pGST A2-2	hGST A3-3
Substrate	5AD		CDNB	
Inhibition type	Competitive		Mixed	
$K_i$ , nM	30±3	78±9	22±2	26±2
$\alpha$	$\infty$	$\infty$	5±1	10±4
$k_{\text{cat}}$ , $\text{s}^{-1}$	42±2	223±9	18±1	34±1
$K_M$ , $\mu\text{M}$	73±7	73±7	319±14	640±33
[E], nM	3	1	64	25

## FIGURE LEGENDS:

**Figure 1.** Multiple sequence alignment using CLUSTAL 2.0.12. Boxes outline clusters of different residues in pGST A2-2 in comparison to hGST A3-3. H-site and G-site residues are highlighted in black ■ and white □, while residues contributing to both sites are marked with black/white pattern ▣. Active site residues were deduced from the following PDB entries: for hGST A1-1 – 1GSF (2.70 Å) and 1PKW (2.00 Å); for hGST A2-2 – 2VCT (2.10 Å) and 2WJU (2.30 Å); for hGST A3-3 – 2VCV (1.80 Å) and 1TDI (2.4 Å); for hGST A4-4 – 1GUL (2.70 Å). Secondary structure was visualized by the aid of POLYVIEW [46] using respective PDB entries and aligned as hA3-hA1-hA2-hA4 from top to bottom above the amino acid sequences.

**Figure 2.** Comparison of  $k_{cat}/K_M$  values of pGST A2-2, hGST A1-1 and hGST A3-3. Structures of substrates used for characterization are presented to the right. Double-headed arrows represent maximal and minimal values when the bar is an average of several values.  $k_{cat}/K_M$  values for human GSTs are taken from the literature: hGST A1-1 [11, 15, 29, 30, 47-49] and hGST A3-3 [15, 21, 29, 34, 50]. Asterisks represent estimated values based on available specific activities.

**Figure 3.** Tissue-specific expression of pGSTA2. **(A)** Cloning of pGST A2-2 from ovary and testis reveals comparably high amounts of pGSTA2 cDNA. The molecular cloning of pGSTA2 was performed in parallel from ovary and testis. The same amount of mRNA cDNA template was used for final PCR intended for full-length pGSTA2 cDNA. Similar amounts of pGSTA2 cDNA are obtained from ovary and testis. **(B)** Full-length pGSTA2 cDNA from ten tissues was amplified using sequence specific primers. Primers to amplify porcine  $\beta$ -actin were designed to exclude  $\alpha$ -actin and non-spliced isoforms of  $\beta$ -actin. Intensity of PCR fragments was evaluated using Image J 1.33u software (NIH). For quantification, pGSTA2 PCR fragment intensities were normalized to the respective  $\beta$ -actin band intensities. The resulting intensities were further normalized to pGSTA2 band intensity in liver. Final normalized intensities were assigned to ordinal scale as follows: (0; 0.1) = +, [0.1; 0.5) = ++, [0.5; 1) = +++.

**Figure 2.****Figure 3.**

THIS IS NOT THE VERSION OF RECORD - see doi:10.1042/BJ20100839